Parasitol Res (2009) 105:237–248
DOI 10.1007/s00436-009-1387-z

ORIGINAL PAPER

Schistosoma japonicum: proteomics analysis of differentially expressed proteins from ultraviolet-attenuated cercariae compared to normal cercariae

Lin-lin Yang · Zhi-yue Lv · Shao-min Hu · Si-jie He · Zheng-yu Li · Shuang-min Zhang · Huan-qin Zheng · Ming-tao Li · Xin-bing Yu · Ming-Chiu Fung · Zhong-dao Wu

Received: 4 December 2008 / Accepted: 27 February 2009 / Published online: 17 March 2009

Abstract Schistosomiasis is considered the most important human helminthiasis in terms of morbidity and mortality. In this study, comparative soluble proteomic analysis of normal cercariae and ultraviolet-irradiated attenuated cercariae (UVAC) from *Schistosoma japonicum* were carried out in view of the high efficiency of irradiation-attenuated cercariae vaccine. The results revealed that some proteins showed significant differential expression in the parasite after treatment with ultraviolet light. Total 20 protein spots were identified by mass spectrometry, corresponded to five groups according to their functions in the main that were structural and motor proteins (actin, et al.), energy metabolism associated enzymes (glyceraldehydes-3-phosphage dehydrogenase, et al.), signaling transduction pathway-associated molecules (14-3-3 protein, et al.), heat shock protein families (HSP 70 family, et al.), and other functional proteins (20S proteasome). Furthermore, our results indicated that the differential expression of the proteins by ultraviolet irradiation may be, at least partially, acquired by regulating the mRNA levels of corresponding proteins. These results may provide new clues for further exploring the mechanism of protective immunity induced by UVAC and may shed some light on the development of vaccines against schistosomiasis.

Lin-lin Yang and Zhi-yue Lv made the same contribution to this work.

L.-l. Yang · Z.-y. Lv · S.-j. He · Z.-y. Li · S.-m. Zhang · H.-q. Zheng · X.-b. Yu · Z.-d. Wu
Department of Parasitology, Zhongshan School of Medicine, Sun Yat-sen University, 74 2nd Zhangshan Road, Guangzhou 510089, China

L.-l. Yang · Z.-y. Lv · S.-j. He · Z.-y. Li · S.-m. Zhang · H.-q. Zheng · X.-b. Yu · Z.-d. Wu (✉)
Key Laboratory for Tropical Diseases Control, The Ministry of Education, Sun Yat-sen University, Guangzhou 510089, China
e-mail: wuzhd@mail.sysu.edu.cn

S.-m. Hu · M.-C. Fung
Department of Biology, The Chinese University of Hong Kong, Hong Kong, China

M.-t. Li
Proteomics Laboratory, Zhongshan School of Medicine, Sun Yat-sen University, 74 2nd Zhongshan road, Guangzhou 510089, China

Introduction

Schistosomiasis is a serious parasitic zoonosis caused by blood-dwelling flukes of the genus *Schistosoma*. It is endemic in 76 countries and at least 600 million people are currently at risk of infection and 200 million are infected (WHO 2002). At present, morbidity control with chemotherapy is the predominant intervention method against schistosomiasis on the recommendation of WHO since 1984. However, population-based treatment with praziquantel requires a substantial infrastructure to cover all parts of an endemic area regularly, and rapid reinfection following treatment makes chemotherapy expensive. In addition, expanded chemotherapy programs may carry with them the specter of drug resistance (Bergquist and Colley 1998). Thus, continued research on the development of schistosome vaccines and new drug targets remain the priority to potentially control this major parasitic disease.

For more than 80 years, efforts have been made to develop a vaccine against schistosomes. But, unfortunately, we fail to

obtain any genuinely effective vaccines at present. In 1990s, WHO/Research and Training in Tropical Diseases selected six vaccine candidate molecules of *Schistosoma mansoni* to undertake independent mouse studies in parallel (Bergquist 1995). However, none of them has been able so far to give a consistent induction of more than 40% protection. The studies of testing irradiation-attenuated cercariae as a possible vaccine against schistosomiasis were performed more than 50 years ago (Villella et al. 1961; Szumlewicz and Olivier 1963). Many studies have shown that administration of live irradiation-attenuated cercariae to a large range of laboratory animals (Ruppel et al. 1990; Shi et al. 1990, 1993), including nonhuman primates (Shi et al. 1993; Eberl et al. 2000; Torben and Hailu 2007), could provide 70–90% protection against experimental *S. mansoni* and *Schistosoma japonicum* infections. But due to the limit of cercariae supply and transportation and ethical implications for using living parasites, it is not feasible to use irradiated cercariae as vaccine in humans. In spite of that, the irradiated cercariae vaccine provides us a rational model that enables dissection of the mechanisms of the induced protective immunity (Mountford and Harrop 1998).

With the advent of proteomic techniques, the extensive expressed sequence tag (EST) sequencing and the release of the draft genome assembly of S. *mansoni* and *S. japonicum*, it is now possible to identify individual proteins that are differentially expressed in the ultraviolet-irradiated attenuated cercariae (UVAC). In the present study, we explored the proteins that are differentially expressed between normal and UV-irradiated cercarial bodies by two-dimensional electrophoresis (2-DE) followed by protein identification via mass spectrometric (MS) methods, which may uncover molecules that help to understand the mechanism of attenuated cercariae-induced protective immunity and provide further insight into the development of antischistosomiasis vaccines.

Materials and methods

Parasite maintenance

A Chinese mainland strain of *S. japonicum* was used in the experiment. Infected *Oncomelania hupensis* snails were obtained from Institute of Schistosomiasis Control, Hunan, People's Republic of China and maintained in the laboratory under controlled conditions.

Cercariae were shed from host snails, and the cercarial bodies were transferred into a 50-ml centrifuge tube with Earle's buffer (HyClone, Logan). For irradiated attenuation, the cercarial bodies were exposed to a UV source (Cole-Parmer, USA) with 254 nm wavelength at an intensity of 400 μW/cm^2 for 1 min (Shi et al. 1990). All cercarial bodies were harvested and washed with cold sterilized Earle's buffer for three times then were transferred to six-well plates containing complete growth medium Rapid Prototyping and Manufacturing Institute-1640 (Gibco, USA) supplemented with 10% FBS (Gibco), 100 μg/ml penicillin, and 100 μg/ml streptomycin and incubated at 37°C under 95% humidity for 3 days. After incubation, the cercarial bodies were harvested by centrifugation at 150×*g* for 20 min and washed with chilled phosphate buffered saline for three times. The parasite pellets were resuspended in 1 mM phenylmethylsulphonyl fluoride (Amersham Biosciences, UK), snap-frozen in liquid nitrogen, and stored at −80°C.

Preparation of soluble protein extracts for 2-DE

To avoid further purification after sample extracting and loss of protein during the two-step equilibration after first-dimension isoelectric focusing (IEF), protein samples were prepared by the method of "pre-reduction alkylation" (Herbert et al. 2001). Frozen parasite samples were thawed on ice and resuspended in prereduction alkylation lysis buffer containing 7 M urea (Amersham Biosciences), 2 M thiourea (Sigma, UK), 2% 3-3-cholamidopropyl-dimethylammonio-1-propanesulfonate (CHAPS; Amersham Biosciences), 20 mM trishydroxymethylaminomethane (Tris; Amersham Bio sciences), 5 mM tributyl phosphate (Sigma), and 0.5% immobilized pH gradients (IPG) buffer (pH 3–10, Amersham Biosciences) which were added freshly before use. Thawed samples were homogenized with an electric homogenizer on ice and then incubated at room temperature for 15 min to let them dissolve completely. More intensive disruption of soluble protein was achieved by sonication (5×30 s bursts at 37% intensity) with intervals of 1 min on ice between bursts to prevent overheating. The extracts were incubated at room temperature for 2 h and then centrifuged for 1 h at 20,000×*g*, 4°C, to remove the insoluble materials. The supernatant containing soluble proteins was collected as the crude protein sample. Of iodoacetamide (Sigma) stock solution, 200 mM was added into the extracted supernatant to a final concentration of 20 mM and incubated at room temperature for 1.5 h in the dark. A fourfold volume of acetone precooled at −20°C was then added and incubated at −20°C overnight to precipitate the proteins. Protein pellets were obtained by centrifugation at 12,000×*g* for 30 min, 4°C, then dried and resuspended in rehydration buffer containing 7 M urea, 2 M thiourea, and 2% CHAPS. The protein concentration was determined with the 2-D Quant kit (Amersham Biosciences) according to the manufacturer's instructions.

Electrophoresis

Three gels were prepared for each sample of soluble proteins from normal and UV-irradiated cercarial bodies. The 2-DE was based on Görg et al. (2000) where first-dimension IEF

was performed in 24 cm linear IPG 3–10 strip (IPG-strip; Immobiline Drystrips, Amersham Biosciences). For each gel, 400 μg of protein in each sample was diluted to a final volume of 450 μl with rehydration buffer and 1% bromophenol blue (BPB) solution, 0.5% IPG buffer (pH 3–10) added freshly, and then passively in-gel rehydrated into IPG-strip using Ettan IPGphor II isoelectric focusing system (Amersham Biosciences) at 16°C, 30 V for 12 h. The separation was performed at 500 V for 1 h, followed by a separation over 4 h where the voltage was gradually raised from 1,000 to 8,000 V which was maintained for several hours to give a total of approximately 80 kVh. All isoelectric focusing took place with a maximum current of 50 μA/strip. Upon completion of IEF, the focused first-dimension IPG-strips were proceeded to gel equilibration immediately prior to the second-dimension separation.

Because proteins had been reduced and alkylated during the extraction step, the strips were equilibrated for 25 min at room temperature following one step equilibration method between the first and second dimension separations, which is done to saturate the IPG-strips in sodium dodecyl sulfate (SDS) equilibration buffer containing 50 mM Tris-HCl (pH 8.8), 6 M urea, 30% (*v*/*v*) glycerol, 2% (*w*/*v*) SDS, and small amounts of BPB for visualization. Six gels were cast and run simultaneously using the Ettan DALTsix electrophoresis system (Amersham Bioscience). Equilibrated IPG-strips were applied onto the top of the second-dimension polyacrylamide gels and sealed with 0.5% (*w*/*v*) agarose dissolved in 1× cathode buffer (Amersham Bioscience), together with the low molecular weight protein marker (Amersham Bioscience). Proteins were separated across 20× 24×0.1 cm, 12.5% SDS-polyacrylamide gel electrophoresis (PAGE), and electrophoresis was performed at 16°C at a maximum current of 40 mA per gel, 2 W/gel for 50 min in the first step, followed by 100 W for total six gels until the BPB reached the bottom of the gel.

Protein visualization

Gels were stained using the improved silver-staining method compatible with matrix-assisted laser desorption/ionization-time of flight (MALDI-TOF) MS based on the European Molecular Biology Laboratory silver-staining method (Mortz et al. 2001). Briefly, the gels were first fixed in 50% methanol and 5% acetic acid (*v*/*v*) for 40 min, then washed in 50% methanol for 20 min, and afterward rinsed in Milli-Q water overnight to reduce background staining as far as possible. The sensitization was performed in 0.02% sodium thiosulfate for 2 min, followed by staining in 0.1% silver nitrate for 40 min. The color was developed in 2% (*w*/*v*) sodium carbonate with 0.04% (*v*/*v*) formaldehyde and stopped with 5% acetic acid. Between each step, the gels were rinsed with Milli-Q water for three times to reduce background staining. The stained gels were stored at 4°C in 1% acetic acid for further visualization.

Image scanning and analysis

Silver-stained gels were scanned at 300 dpi, 12-bit gray scale, with green color filter, using Labscan (Amersham Biosciences) in transmission mode and the images were sent to ImageMaster 2D Platinum v5.0 software (Amersham Biosciences) for direct analysis. Protein spots were automatically detected firstly after adjustments of smooth parameter, saliency value and minimum area value to remove high noise spots and intense artifact spots. Minimal manual editing to remove obvious artifacts and delete, split, or redraw poorly assigned spots were performed to make the detecting more accurate. A reference gel containing maximum spots was selected from one of the normal gels that set to compare with other gels together with some landmarks between all gels created manually for seed matching. Unmatched proteins spots of the member gels were automatically added to the reference gel. After automatic matching of spots, followed again with minimal intervention to correct some matches and unmatches, especially the differential spots, the individual protein spot quantity was presented as a percentage of its normalized volume corresponding to the area and intensity of all spots detected in the gels (vol.% value) in spite of potential experimental variations between gels that are caused by difference in the amounts of protein loading or inequalities in staining and exported to Excel (Microsoft Office) for further analysis.

In-gel digestions and MS analysis of selected protein spots

The pick list of selected protein spots was exported to Ettan Spot Handling Workstation (Amersham Biosciences) which carried out robotically the spot picking, destaining, digestion, extraction, MALDI sample preparation, and spotting on MALDI target trays. Briefly, gel plugs robotically picked into 96-well microplates were rinsed by three wash cycles in 1:1 mixture of 30 mM potassium ferricyanide/100 mM sodium thiosulfate to destaining, left to stand for 20 min, and then washed with Milli-Q water until the gels became clear. After equilibration in 50 mM ammonium bicarbonate (Ambic)/50% methanol for 20 min afterward, the excised spots were dehydrated with 75% acetonitrile (ACN) for 10 min, following by drying in a heated air circulating drying module for another 10 min. To the dried plugs, 10 μl of digestion solution (40 ng/μl sequencing grade trypsin, Promega, USA, in 20 mM Ambic) was added and the plates were transferred to the digestion station for incubation at 37°C for 1 h. The resulting peptides were subsequently extracted twice from the gel pieces with extraction solution (50% ACN containing 0.1%

trifluoroacetic acid (TFA)) and the supernatants were transferred into new 96-well microplates that were evaporated to dryness. MALDI samples were prepared by reconstituting the dried peptides in 5 μl of 50% ACN containing 0.5% TFA. A 0.3-μl sample was applied to the clean MALDI sample slide surface and allowed to dry at room temperature, repeated for three times. The spots were then redissolved by the addition of 0.3 μl of saturated matrix solution (α-cyano-4-hydroxycinnamic acid saturated solution in 50% ACN containing 0.5% TFA) and finally introduced into the MALDI-MS after drying.

MS was performed using an Ettan MALDI-TOF mass spectrometer (Amersham Biosciences) in the Proteomic laboratory of Sun Yat-sen University (GuangZhou, China). MALDI peptide mass fingerprinting was carried out in positive ion reflector mode. Internal calibration was performed using the autodigest peaks of trypsin at *m/z* 842.509 and 2,211.104. Each spectrum corresponded to an average of 200 laser shots, with an accelerating ion source voltage of 20 kV, N2 laser of 337 nm, 200 ns delay, and mass gate from 600 to 3,500*m/z*. Protein identifications by peptide mass fingerprinting (PMF), the resulting spectrum after excluding the contaminant and adduct peaks from the created peak list, were carried out by searching the National Center for Biotechnology Information nonredundant (NCBInr) protein database and Swiss-Prot database using Maldi evaluation V2.0 software (Amersham Biosciences) via MASCOT search engine (http://www.matrixscience.com/cgi/search_form.pl?FORMVER=2&SEARCH=PMF). The search parameters included a peptide mass tolerance of ±100 ppm, a maximum of one missed tryptic cleavage site, minimum signal–noise ratio of 2.5, fixed modifications of alkylation of cysteine by carbamidomethylation, oxidation of methionine as possible modifications, and taxonomy filter of "metazoan" species. A protein was considered to be identified when two or more peptides with confidence interval above 99% were positively matched in the database.

Real-time fluorescent quantitative reverse transcription PCR analysis of four differentially expressed proteins

Four identified proteins were chosen for further analysis on the mRNA level using real-time fluorescent quantitative polymerase chain reaction (RT-FQ-PCR). Cercarial bodies were collected and treated as described above. Ultraviolet-irradiated cercarial bodies were prepared after four doses of ultraviolet irradiation (400, 300, 200, or 100 μW/cm^2, respectively, for 1 min) and cultured for 1 or 3 days before RNA isolation. Total RNAs were then isolated by Trizol reagent (Invitrogen, USA) with an RNase free DNase treatment for 30 min afterward. According to the manufacturer's instructions, the RNAs were reverse transcribed to cDNAs using random oligo $(dT)_9$ primers (9 mer, TaKaRa, Japan) and ReverTra Ace Moloney murine leukemia virus reverse transcriptase (Toyobo, Japan). Reverse transcription was performed for 60 min at 42°C, followed by denaturation at 95°C for 5 min. Specific primers were designed for RT-PCR analysis with Primer Express software (Applied Biosystems, USA) as follows: actin (GenBank accession no. AF223400), forward primer 5′ GAAGGTTATGCTCTGC CACATG 3′ and reverse primer 5′ AAGCTGTAACCA CGCTCAGTCA 3′; alcohol dehydrogenase (ADH, GenBank accession no. AY815468), forward 5′ TGTACATCCTGGTG CAGTCAGAA 3′ and reverse 5′ GAGCACCTTCCCATG GACTTAT 3′; heat shock protein 70 (HSP70, GenBank accession no. AY813185), forward 5′ TGTAGCCGCGCGT GATAA 3′ and reverse 5′ CATTGCG CACCATATTTTCG 3′; and beta-tubulin (GenBank accession no. AY220457), forward 5′ CGGCCGTTTGCGATATACC 3′ and reverse 5′ CTGCTCGGATACACGCTTGA 3′. The amplification fragments were 100 bp in length. Variability in gene expression resulting from disparities in parasite numbers or RNA isolation efficiency was normalized by amplification of a constitutively expressed reference gene, 18sRNA (GenBank accession no. DQ442999) to calculate the levels of target genes (Schmittgen and Zakrajsek 2000). The specific forward primer 5′ CCACACGTGCGCTA CAATG 3′, and reverse primer 5′ AGTTTGCCCAACCC TTTCG 3′ amplified a 67-bp fragment.

The real-time quantitative RT-PCR assays were carried out on the ABI PRISM 7000 sequence detecting system (Applied Biosystems) using the sequence unspecific SYBR Green I. Quantitative standards of each gene were made using the previous PCR products as the templates with every tenfold dilution, and the efficiency of amplification of each fragment can be calculated from the standard curve. Each amplification was performed in triplicate wells. The reactions included 2 μl of the reversed transcribed cDNA, 0.4 μmol of each primer, and the SYBR Green Realtime Master Mix (Toyobo) in a total volume of 50 μl. The PCR was performed under the following cycling conditions: an initial denaturation step at 93°C for 5 min, followed by 40 cycles of amplification of additional denaturation at 93°C for 1 min, annealing at 53°C for 1 min, and extension at 72°C for 1 min. Template-negative controls and reverse transcriptase negative reactions were run together in order to check for false positive results due to contaminated DNA. After PCR, all of the final PCR products were detected by melting curve analysis which was subsequently performed by increasing the temperature slowly from 60°C to 95°C with a temperature transition rate of 0.1°C/s and measuring the fluorescence continuously. The differences in melting temperature of PCR produces allowed to distinguish the genuine products from potential remaining primer

dimers and any nonspecific products. The ABI PRISM 7000 SDS software (Applied Bioscience) was used for the analysis and interpretation of the results. The amount of induction of mRNA was determined from the threshold cycle values and the comparative threshold cycle ($2^{-\Delta\Delta CT}$) method was used to allow the semiquantification (Livak and Schmittgen 2001). All data were from experiments performed at least three times and analyzed using Student's *t* test to compare the expression of each gene between the eight irradiated cercariae groups and normal cercariae (NC) group.

Results

2-DE separations of soluble proteins from NC and UVAC

The soluble proteins from NC and UVAC were analyzed by 2-DE to determine whether certain proteins were differentially or uniquely expressed during the attenuation. Two sample preparations of total protein extracts, one from ultraviolet-irradiated cercarial bodies and the other from normal cercarial bodies, were used to develop proteomic maps. The protein expression profiles of whole soluble protein extract from two preparations were reasonably well represented by 2-DE separations (Fig. 1), across a gradient of pH 3–10. Taking the analytical software parameters setting for "real" spots into account, only about 1,000 spots were detected from over 2,000 putative spots in each gel. Triplicate gels of each sample preparation were produced in view of gel-to-gel variation. In total, on average 1,458±29 and 1379±45 spots were respectively detected from NC and UVAC, most of which concentrated at the range between 22 and 95 kDa with the theoretical pI varying from 4 to 8 (data not shown). Gels between the two preparations groups were very similar with matches reaching 83.6%, indicating similarity in expression of most proteins and difference in only a few of the proteins. Most unmatched spots are proteins with low-abundance represented below 30 kDa and with extremely alkaline pI or acidic pI which makes it difficult to separate them clearly (data not show).

Comparison of protein spots in maps

The silver-stained 2-DE gels were scanned with Labscan, and the digital images were analyzed by ImageMaster 2D software (version 5.0). Corresponding spots on each of the triplicate gels were compared for variation within its respective group, and spot intensity mean values were then compared between irradiated and normal groups to investigate any different expression profiles. A change above 1.5 folds in spot quantity was considered significant. These

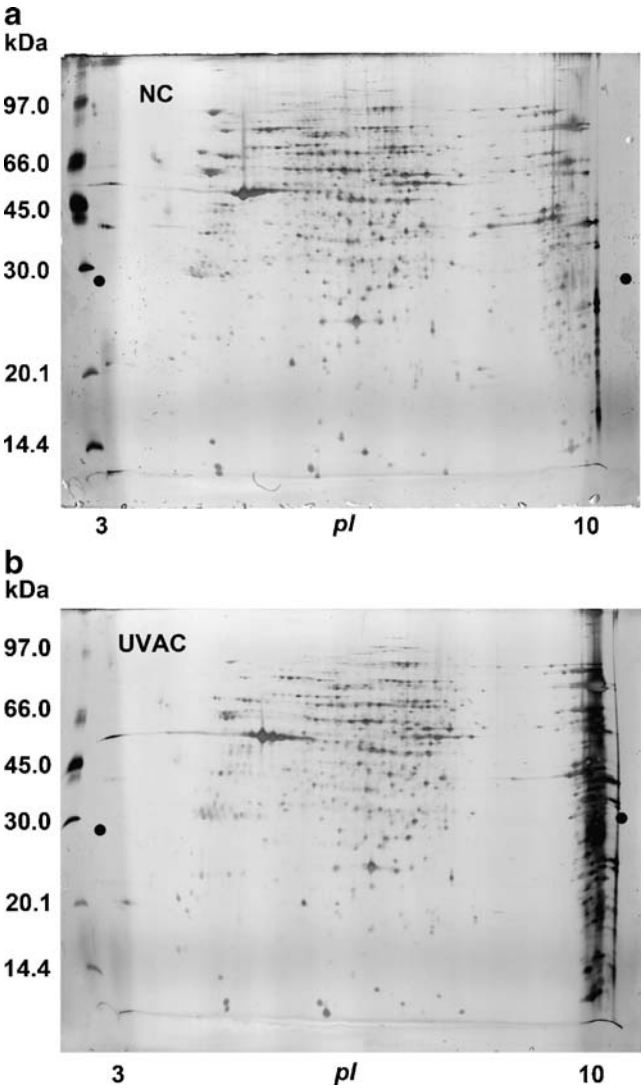

Fig. 1 Separation of total soluble proteins extracted from normal cercariae (*NC*) and UV irradiation-attenuated cercariae of *S. japonicum* on silver-stained two-dimensional electrophoresis gels over the pH range 3–10. Each gel is representative of three replicated gels. Twenty protein spots that have been positively identified by MS are listed in Table 1 with index number and corresponding details

comparisons revealed that four spots were detected only in the UVAC gel and eight spots were uniquely represented in NC gel. A total of nine proteins were upregulated in UVAC gels, while 38 proteins showed a lower expression compared to normal control. Representative examples of these differentially expressed proteins spots of the 2-DE gels from NC and UVAC identified by MALDI-TOP MS are shown in Fig. 2.

MS analysis of differentially expressed proteins

Since some spots that show differential expression were present in insufficient quantities for MS analysis, only a total

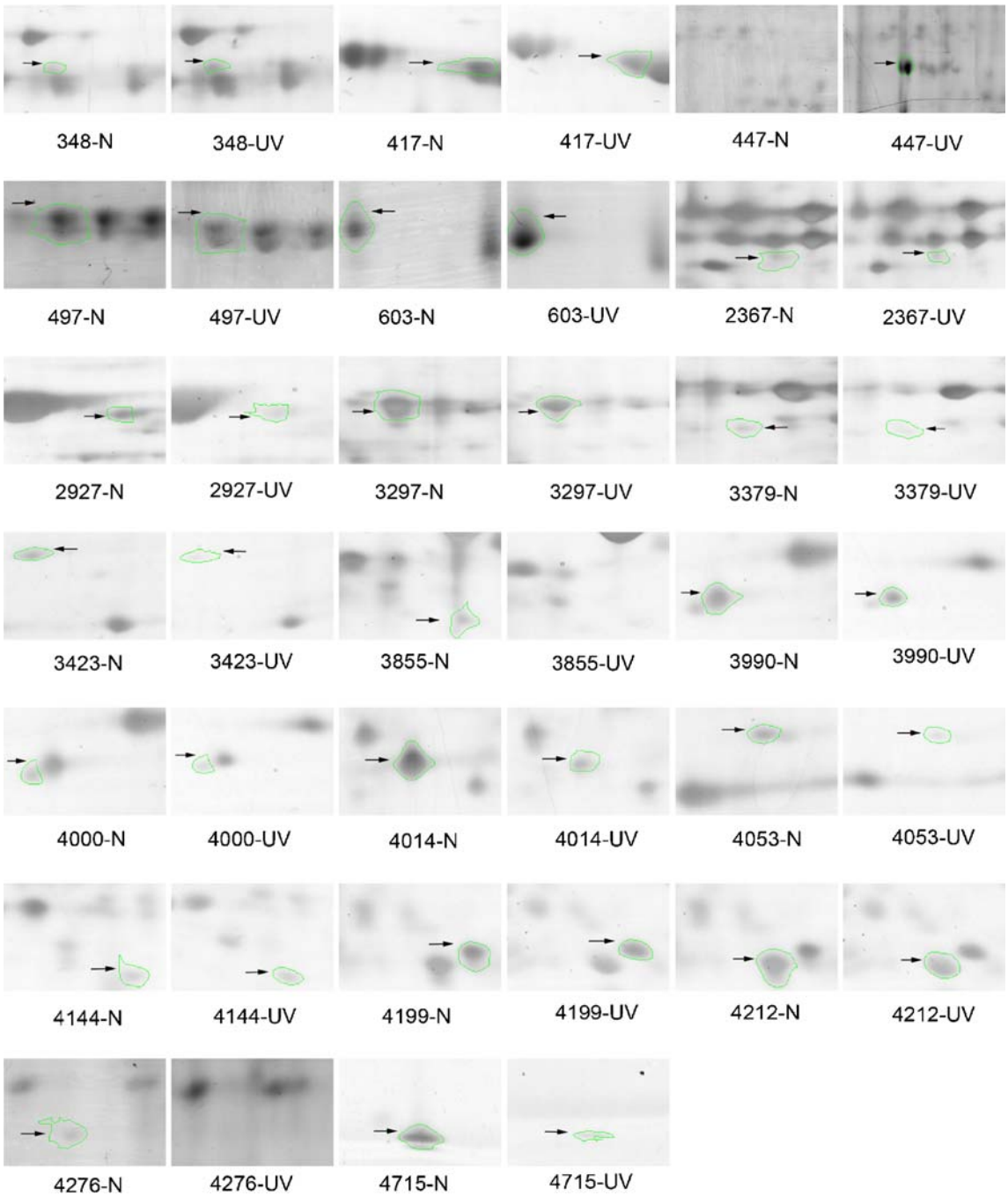

Fig. 2 Subsection views of the differentially expressed protein spots on the two-dimensional gels of UV-irradiated (*UV*) and normal (*N*) cercarial bodies from *S. japonicum*. *Arrowheads* indicated the spots identified by MALDI-TOF-MS. The *individual spot number* is marked as showed on the reference gels of normal cercariae

of 46 differentially expressed protein spots were selected for identification, four spots uniquely expressed in irradiated cercarial bodies, eight uniquely expressed in normal cercarial bodies, nine upregulated and 25 downregulated in irradiated cercarial bodies. However, only 20 spots were successfully identified by MALDI-TOF MS for PMF (details shown in Table 1). A representative PMF map of spot 3,855 is shown in Fig. 3. The PMF results were used to search the NCBInr by Maldi evaluation software and then search the Swiss-Prot databases via Internet. One and two unique proteins were respectively identified for the irradiated cercariae and normal cercariae and three upregulated and 14 downregulated proteins for the irradiated cercariae. Additionally, two spots were identified as actin, of which one was only found in UV-irradiated cercariae group while one was downregulated in UV-irradiated cercariae group.

Table 1 Overview of proteins identified by MALDI-TOF analyses that showed significant differential expression between normal cercariae and UV-irradiated cercariae

Spot ID[a]	Protein name	NCBI accession ID no.	Functional clustering[b]	MW (kD)[b]	PI[b]	Sequence coverage[c]	Species matched	Fold increase[d]
348	Heat shock 70 kDa homolog protein	P08418	Stress response/ chaperone	69.88	5.4	57.5	*Schistosoma mansoni*	1.90534
417	Beta-tubulin	AAO59417	Cytoskeleton	49.62	4.8	45.8	*Schistosoma japonicum*	2.19199
447	Actin	Q9UVX4	Structural protein/ cytoskeleton	41.61	5.3	22.9	*Coprinopsis cinerea*	+
497	Actin	AAF34686	Structural protein/ cytoskeleton	41.74	5.3	65.6	*Schistosoma japonicum*	−2.170608
603	Alcohol dehydrogenase	AAF01711	Carbohydrate/energy metabolism	22.72	7.0	27.8	*Gossypium trilobum*	2.081959
2367	Thiamine pyrophosphate (TPP) family	AAW25278.1	Metabolism	44.46	8.8	32.4	*Schistosoma japonicum*	−2.11257
2927	HSP90 family	AAW27659.1	Stress response/ chaperone	82.71	5	30.2	*Schistosoma japonicum*	−3.12129
3297	HSP60 family	AAW24883.1	Stress response/ chaperone	62.64	9.7	14.6	*Schistosoma mansoni*	−4.66076
3379	Tropomyosin-2 (TMII)	P42638	Muscle molecular motor	32.68	4.5	40.8	*Schistosoma mansoni*	−3.22677
3423	Calreticulin (55kD antigen)	AAC00515.1	Secretory pathway	46.02	4.5	15.2	*Schistosoma japonicum*	−4.90543
3855	Tropomyosin	AAA88531.1	Muscle molecular motor	33.06	4.6	34.2	*Schistosoma japonicum*	−
3990	Similar to lactate dehydrogenase A	AAP06144.1	Carbohydrate/energy metabolism	32.91	6.7	16.7	*Schistosoma japonicum*	−2.7458
4000	Lactate dehydrogenase-like protein	AAO59420.2	Carbohydrate/energy metabolism	36.49	9.1	18.4	*Schistosoma japonicum*	−1.9775
4014	Glyceraldehyde-3-phosphate dehydrogenase	AAB52408.1	Carbohydrate/energy metabolism	36.9	8.5	21	*Schistosoma japonicum*	−6.05041
4053	Glyceraldehyde-3-phosphate dehydrogenase	BAD06415.1	Carbohydrate/energy metabolism	24.68	8.9	23.5	*Schistosoma japonicum*	−4.03391
4144	Similar to GTP-binding protein beta subunit	AAW26990.1	Signal transduction	38.06	5.6	13.2	*Schistosoma japonicum*	−1.93767
4199	Similar to proteasome subunit, alpha type 5	AAP06025.1	Proteolytic enzyme	27.48	5.2	34.3	*Schistosoma japonicum*	−1.75102
4212	Similar to 14-3-3 protein	AAP06477.1	Signal transduction	28.59	5.2	28.5	*Schistosoma japonicum*	−1.84053
4276	similar to proteasome_beta_type_3	AAW25726.1	Proteolytic enzyme	21.23	5.9	32.6	*Schistosoma japonicum*	−
4715	Dynei light chain 1	AAD41631.1	Muscle molecular motor	10.56	6.5	75.3	*Schistosoma japonicum*	−2.3977

+ spots that uniquely detected in the irradiated cercariae, − spots that not detected in the irradiated cercariae

[a] The Spot ID were determined when spots were detected at the beginning of analysis of gels

[b] The functions are cited from protein database (NCBInr) remarks and the calculated MW and pI as recorded in the database also

[c] Protein database entries identified by peptide mass fingerprinting. The percentage coverage is defined as the ratio (%) of the protein sequence covered by the matched peptides

[d] Fold increase indicates the difference in normal volume percentage between matched spots from UV-irradiated cercariae and normal cercariae. The ratio is the volume percentage value of normal cercariae divided by the value of UV-irradiated cercariae

RT-FQ-PCR analysis of four differentially expressed proteins in mRNA level

To study whether the UV irradiation-induced differential expression of the identified differentially expressed proteins happen in the mRNA levels, four proteins ADH, HSP70, beta-tubulin, and actin were chosen for real-time quantitative RT-PCR analysis. These proteins have been identified as unique expressed spots in 2-DE analysis (Fig. 2. 603 N and 603 UV for ADH, 348 N and 348 UV for HSP70, 417 N and 417 UV for beta-tubulin, and 447 N and 447 UV for Actin). High efficiencies of amplifications of these five PCR reaction

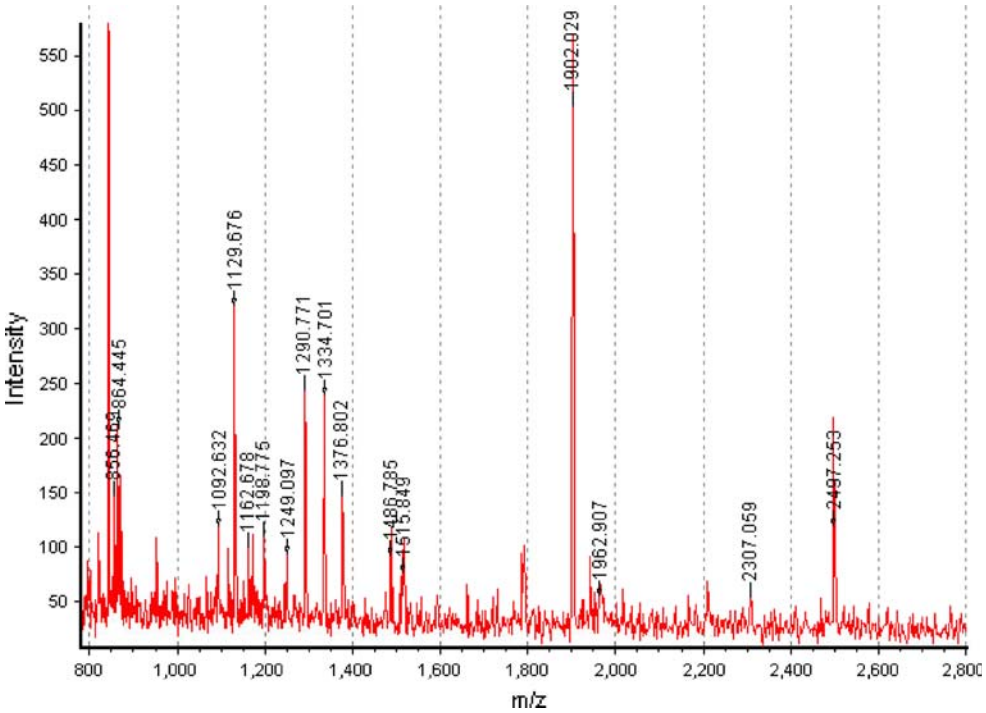

Fig. 3 A representative peptide mass fingerprinting of protein spot 3855 (*S. japonicum* tropomyosin)

systems were obtained indicated by the standard curve slopes approaching the value of −3.32 for every tenfold dilution of each target (data not shown), which allowed the fold change values to be determined after normalization of each gene to internal control s18RNA using the comparative threshold method. The results indicated that 24 h after ultraviolet irradiation at 400 μW/cm^2 for 1 min, the mRNA levels of ADH, beta-tubulin, HSP70, and actin were significantly upregulated in the irradiated groups as compared to the normal group (Fig. 4). The mRNA levels of these four genes in 400 μW/cm^2 ultraviolet irradiated cercarial bodies decreased rapidly but retained higher than those of normal groups 3 days after treatment (Fig. 4). These results corresponded to our observation of 2-DE analysis (Table 1) and therefore indicated that the ultraviolet irradiation-induced differential expression of these identified proteins may be mainly regulated in the mRNA level.

As previous studies indicated that the dosage of ultraviolet could affect the protective effect of attenuated cercariae, 300–455 μW/cm^2 have been thought to be optimal and thus widely used for the attenuation of *S. japonicum* cercariae (Ruppel et al. 1990; Shi et al. 1993). We therefore sought to investigate the effects of the dosage of ultraviolet irradiation on the mRNA levels of the ADH, HSP70, beta-tubulin, and actin. Our results indicated that the mRNA levels of these genes were much upregulated 24 h after the cercarial bodies were exposed to 400 or 300 μW/cm^2 ultraviolet irradiation (Fig. 4). However, when the cercarial bodies were exposed to 200 μW/cm^2 ultraviolet irradiation, the mRNA levels of these genes except HSP70 were significant lower than those exposed to 400 or 300 μW/cm^2 ultraviolet (Fig. 4). There were no significant upregulation of the mRNA levels of actin, HSP70, and beta-tubulin in the cercariae 24 h after 100 μW/cm^2 ultraviolet irradiation.

Discussion

To date, over 100 different antigens have been identified, isolated, or cloned and expressed (Bergquist et al. 2002), but yet no one has been able to consistently induce high resistance as effective as sterile immunity stimulated by vaccination with attenuated cercariae. Cercariae attenuated either by gamma-irradiation or UV irradiation can induce high levels of protective immunity in experimentally vaccinated rodents and primates (Ruppel et al. 1990). In view of the protective potential of the irradiated cercariae model, the whole protein expression profile of attenuated cercariae must contain the information that we need to explore the molecular mechanism of this UV-irradiated vaccine. In the present study, we investigated differences of protein expression comparing the UVAC to NC and therefore were able to define distinct total protein pattern changes in UVAC and normal controls.

In recent years, the proteomic approach has been successfully applied to schistosome analysis in proteome components analysis (Curwen et al. 2004; Knudsen et al. 2005; Cass et al. 2007) or novel proteins investigation (Curwen et al. 2006). In this study, we adopted 2-DE and MS techniques for protein identification. As far as we know, this report constitutes the first utilization of proteomics comparing the total soluble body proteins from UVAC

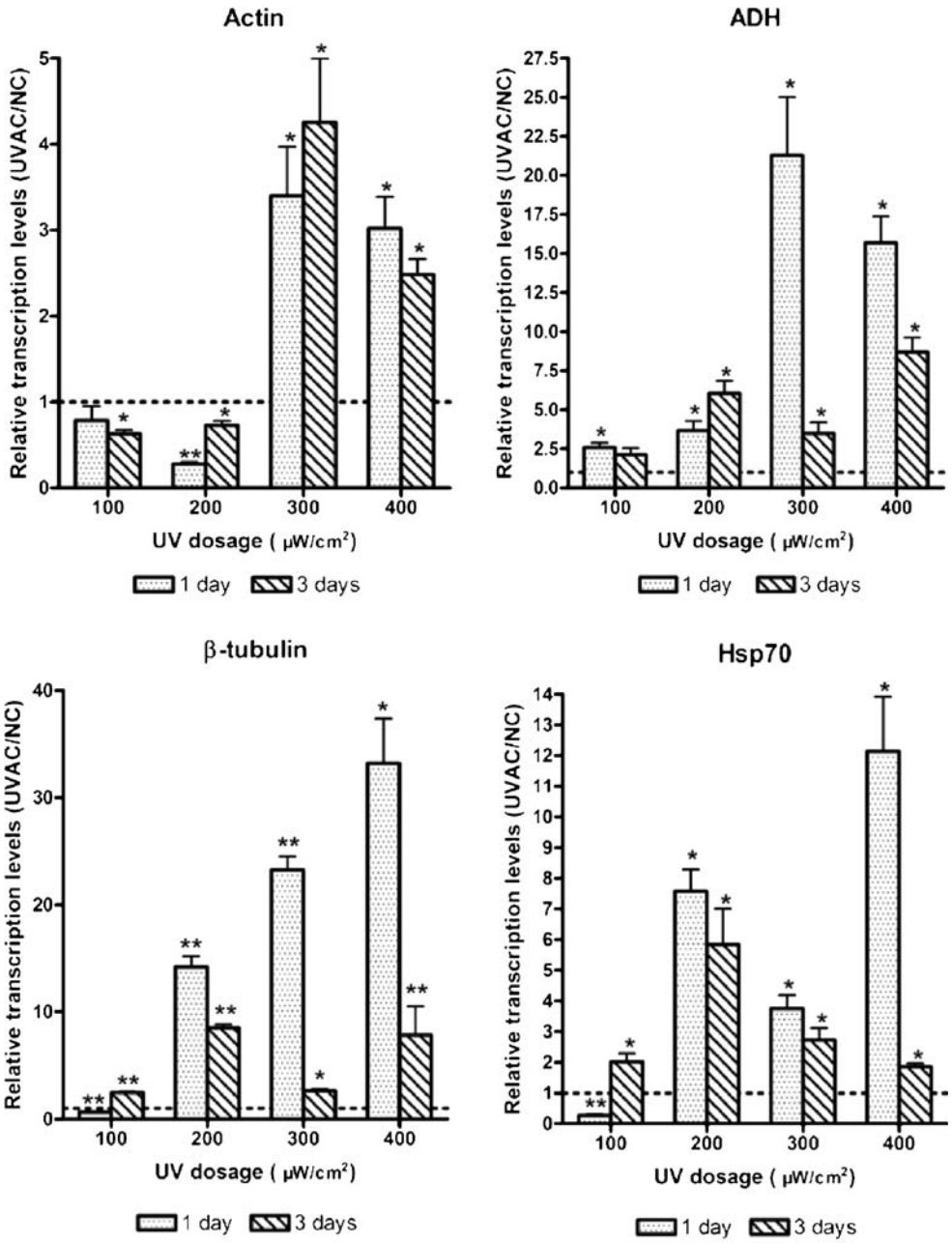

Fig. 4 Real-time quantitative RT-PCR analysis of ADH, beta-tubulin, HSP70, and actin expression in normal cercariae and UV-irradiated cercariae. The transcripted cDNA from total RNA samples prepared from irradiated cercariae under different dosage of ultraviolet and normal cercariae that cultured for different time were used as the template for PCR. Quantitative real-time PCR was performed using gene-specific primers and SYBR Green Realtime Master Mix. The relative gene expression was evaluated using comparative cycle threshold method with 18s RNA as the reference gene and the fold change was determined with the ABI PRISM 7000 SDS software. Means from three independent experiments are shown, and *bars* indicated standard error of the mean obtained from three amplification experiments using independent RNA preparations. *$p \leq 0.1$; **$p \leq 0.01$. *Dotted lines* represent one across *Y*-axis, relative transcription levels (UVAC/NC)

and NC. As the total soluble fractions gave high protein yields and the silver-staining method offers the maximal sensitivity, our proteomic maps revealed 1,458±29 and 1,379±45 spots from normal and irradiated cercarial bodies, respectively (Fig. 1), which was considerably similar with previous studies that identified 1,181 protein spots from cercariae of *S. japonicum* (Liu et al. 2006). For more critical quantitative comparison of spots between different gels by silver staining, we carefully controlled the developing time to avoid producing saturated spots of high concentrated proteins, at the same time ensured as many as possible spots to be developed. Many studies have revealed that the protein synthesis or mRNA transcription of cercariae/schistosomula is inhibited after irradiation (Wales et al. 1992; Charmy et al. 1997), but no significant qualitative differences have been observed using one-dimensional PAGE. Our 2D result showed that 46 spots, out of the total of 59 differentially expressed spots, were downregulated in UV-irradiated cercariae. For MS analysis, PMF were acquired by MOLDI-TOF MS. Despite the fact that a large number of ESTs derived from *S. japonicum* have been released to GenBank (Hu et al. 2003), we regrettably showed that PMF was of limited use for comprehensive protein identification, because it was not

sensitive enough to unequivocally identify a protein. In addition, another technical limitation was that the silver-staining method is not perfectly compatible to MS detecting. Thus, out of total 46 spots picked, only 20 spots were clearly identified within a single spot.

Many arguments have been put forward that it might be multimechanisms involved in multimolecules that priming the immunity in UV irradiation-attenuated cercariae vaccinated animals. In our study, we found five classes of cercarial proteins were differentially expressed after UV irradiation.

One class is cytoskeleton and mobility related molecules, including major components of the microtubular and actin-based cytoskeletal system actin and tubulin which upregulated and microtubule-associated motors tropomyosin and dynein light chain that downregulated. In schistosomes, movement is accomplished through well-developed muscular arrangements that are mainly constructed from tubulin and actin molecules (Mair et al. 2003). The upregulation of these molecules may potentially change the relatively complex muscle organization within the body wall and have detrimental effects on movement, which consistent with the presumption that the delayed migration of attenuated larvae in the skin could lead to great amount of material from the parasite accumulated and stimulate an optimal protection (Riengrojpitak et al. 1998). Tropomyosin and dyneins are both important motors closely related with actin and tubulin involved in various aspects of cell motility (Hoffmann and Strand 1996), and SjDLC is also found to be closely involved and upregulated in the transformation of cercariae to schistosoma (Hoffmann and Strand 1996, 1997). We deduce that the decreased expression of these proteins likely leads to the inhibition of the muscular system movement and contributes to the retarded migration of cercariae in vivo; additionally, the decreased expression of DLC may contribute to destruction of the integrity of the tegument of transformed schistosomula consequently affecting their maturation and continued survival.

The second class is the energy metabolism related enzymes. Four different metabolic enzymes were identified in our work. Glyceraldehyde-3-phosphate dehydrogenase (GAPDH), lactate dehydrogenase (LDH) and a thiamine pyrophosphate (TPP) family molecule were downregulated, while ADH was upregulated. GAPDH is an essential enzyme of the glycolysis energy metabolism pathway. LDH and TPP family proteins are key molecules of the anaerobic metabolism and the tricarboxylic acid cycle, respectively. The inhibition of their expression is deduced to suppress the metabolism of UV-irradiated cercariae and therefore their viability. ADH is a NADP-dependent enzyme that converts pyruvate to ethanol via acetaldehyde (Bruchhaus and Tannich 1994). Its upregulation may break the balance of metabolism circulation and further effect the parasite survival.

The third is the molecules associated with the transcription/translation machinery and regulatory/signaling functions. A spot similar to the 14-3-3 protein, a spot similar to the GTP-binding protein beta subunit, and a spot identified as calreticulin (CR) were found to be downregulated after UV irradiation. In schistosomes, 14-3-3 protein could take part in the transformation of cercariae to schistosomula (Wiest et al. 1992), and GTP-binding proteins are important part of the transmembrane signaling system and may perform an essential function in the maintenance of the schistosome tegument and regulate the diverse activities of the highly dynamic tegument (Loeffler and Bennett 1996). As a parasite with several hosts, the downregulation of these second signaling transduction related molecules in UV-irradiated cercariae is very likely inhibiting the responses of parasite to the irradiation and causing the cellular homeostasis to become unbalanced, which inevitably lead to a series of abnormal responses. CR that localized in penetration gland cells of cercariae might be secreted or excreted during skin penetration, via regulation of Ca^{2+} levels, thus mediating cercarial invasion and muscle contraction (Khalife et al. 1994). So in addition to its important role in signaling transduction, the downregulation of CR might also influence the penetration and viability of UV-irradiated cercariae.

Additionally, two proteolytic enzymes, the 20S proteasome subunit alpha type 5 and beta type 3 were found to be downregulated. The 20S proteasome is the core complex of ubiquitin-proteasome proteolytic pathway responsible for protein degradation that are naturally unfolded, mutated, or oxygen damaged (Orlowski and Wilk 2003; Guerra-Sa et al. 2005). Though downregulation of subunit alpha type 5 and beta type 3 seems unrelated to the protease activity provided by subunit beta types 1, 2, and 5 (William Castro-Borges et al. 2007), we deduced that maybe the expression of these active subunits are also downregulated that just not identified in present work. In this context, downregulation of the 20S proteasome might contribute to persistence and presentation of these altered immunogenic antigens that are modified under UV irradiation and possibly prime the responses of immunity system of irradiated cercariae vaccine (Wales and Kusel 1992).

The last class is the stress-associated proteins: HSP family. A HSP70 protein homolog and proteins belonging to the HSP90 and HSP60 families are differentially expressed after UV irradiation. In human schistosomes, HSPs are inducibly overexpressed when parasites are exposed to significant levels of stress (Maresca and Carratu 1992; Neumann et al. 1993). HSP70 proteins are considered as the predominant HSP family and play the key

regulatory role in parasite development and pathogenesis (De Jong-Brink 1995). UV irradiation is not only a physiological stress but also a severe biological insult to cercariae. After absorption of radiation energy, a chain of radiochemical and metabolic events occurs in a cascade, which might include the downregulation of important proteins described above in our work. Therefore, the upregulation of HSP70 proteins in UV-irradiated cercariae in our work is a reasonable and expected response against the irradiation attack. Studies have shown pathogen-derived HSP70 is a potent inducer of innate and antigen-specific immunity and could be exploited as a vaccine antigen (Todryk et al. 2000; Zugel and Kaufmann 1999). Furthermore, our group has found that recombinant SjHSP70 could activate dendritic cells and enhanced their antigen presentation capacity (data not shown), same as described by Srivastava 2002), indicating level change of HSP70 in UVAC might be related to the induced higher immune protection and provide new clues for the development of vaccine against schistosomiasis. HSP60 and HSP90 proteins are showed to be downregulated in UV-irradiated cercariae, which is consistent with the postulation of Kusel et al. that the synthesis of heat shock proteins is inhibited in UV-irradiated cercariae, which causes the parasite to release a variety of proteins and glycoproteins with an abnormal conformations (Kusel et al. 1989).

Apart from the 2-DE comparison, we also investigated the expression profiles of four proteins on mRNA levels by real-time quantitative PCR. Our data showed a good consistence between the results of these two methods, as the mRNA levels of these four proteins that were shown to be upregulated after ultraviolet irradiation on protein level (Table 1) were also highly transcribed on mRNA level (Fig. 4). These results may also indicate that the ultraviolet irradiation-induced regulation the cercarial proteins expression is acquired by regulating the mRNA levels of the corresponding genes.

The effect of UV dosage on these genes expression could be categorized after analysis of mRNA level by real-time PCR. For the four upregulated genes, the relative mRNA level was significantly upregulated in the 300 and 400 $\mu W/cm^2$ groups, less upregulated in the 200 $\mu W/cm^2$ group, while no significant changes in the 100 $\mu W/cm^2$ group (Fig. 4), which indicated higher dosage of UV irradiation could cause more changes in mRNA levels of corresponding proteins. This result, which corresponded to previous reports that 300–455 $\mu W/cm^2$ of ultraviolet irradiation, was optimal dosage for the irradiated cercariae to induce effective protective immunity (Ruppel et al. 1990; Shi et al. 1993), therefore suggest that the protective efficiency of ultraviolet-irradiated cercariae may be directly related to the regulation of corresponding genes expression in mRNA level.

Our data reported here have identified a set of proteins that are differentially expressed in the UV-irradiated cercarial bodies from *S. japonicum*. Together, these results suggest that some structural and motor proteins, energy metabolism associated enzymes, signaling transduction pathway associated molecules, heat shock proteins, and others with significant roles in the cercariae were changed after certain dosages of UV irradiation, which to a certain extent could explain the mechanism of protective immunity induction of UV-irradiated cercariae as previously presumed (Hewitson et al. 2005). Besides, based on the studies regarding the regulatory effect of ultraviolet irradiation on the mRNA levels of four identified differentially expressed proteins, our results suggest that, at least partially, the ultraviolet-induced differential expression of certain proteins may be due to its regulatory effect on the mRNA levels of corresponding genes. Furthermore, the results may also indicate that protective efficiency of ultraviolet-irradiated cercariae may be related to the regulation of corresponding genes expression in mRNA level. Together, the results of the present study will bring about new insights about the important biological processes of ultraviolet irradiated cercariae-induced protective immunity and may shed some light on the antischistosomiasis japonicum vaccine.

Acknowledgments We gratefully thank Dr. Bernd Kalinna from the University of Melbourne for revising the manuscript. These experiments comply with the current laws of the China and supported by grants from the National Natural Science Foundation of China (grant no. 30771888), Specialized Research Fund for the Doctoral Program of Higher Education (grant no. 20050558069), China Postdoctoral Science Foundation (no. 20060390748), National High-Tech Research and Development Program of China (863 Program; grant no. 2006AA02Z444, 2007AA02Z153), and Project of Basic Platform for National Science and Technology Resources of the Ministry of Sciences and Technology of China (grant no. 2005 DKA21104).

References

Anonymous (2002) Prevention and control of schistosomiasis and soil-transmitted helminthiasis. World Health Organ Tech Rep Ser 912(i–vi):1–57, back cover

Bergquis NR (1995) Controlling schistosomiasis by vaccination—a realistic option. Parasitol Today 11:191–194

Bergquist NR, Colley DG (1998) Schistosomiasis vaccine: research to development. Parasitol Today 14:99–104

Bergquist R, Al-Sherbiny M, Barakat R, Olds R (2002) Blueprint for schistosomiasis vaccine development. Acta Trop 82:183–192

Bruchhaus I, Tannich E (1994) Purification and molecular characterization of the NAD(+)-dependent acetaldehyde/alcohol dehydrogenase from Entamoeba histolytica. Biochem J 303(Pt 3):743–748

Cass CL, Johnson JR, Califf LL, Xu T, Hernandez HJ, Stadecker MJ, Yates JR, Williams DL (2007) Proteomic analysis of Schistosoma mansoni egg secretions. Mol Biochem Parasitol 155:84–93

Castro-Borges W, Cartwright J, Ashton PD, Braschi S, Guerra Sa R, Rodrigues V, Wilson RA, Curwen RS (2007) The 20S proteasome of *Schistosoma mansoni*: a proteomic analysis. Proteomics 7:1065–1075

Charmy RA, el-Kashef HS, el Ghorab NM, Gad HS (1997) Identification of surface tegumental antigens of normal and irradiated schistosomula. J Egypt Soc Parasitol 27:479–491

Coulson PS, Wilson RA (2001) Cellular and humoral immune responses and protection against schistosomes induced by a radiation-attenuated vaccine in chimpanzees. Infect Immun 69:5352–5362

Curwen RS, Ashton PD, Johnston DA, Wilson RA (2004) The Schistosoma mansoni soluble proteome: a comparison across four life-cycle stages. Mol Biochem Parasitol 138:57–66

Curwen RS, Ashton PD, Sundaralingam S, Wilson RA (2006) Identification of novel proteases and immunomodulators in the secretions of schistosome cercariae that facilitate host entry. Mol Cell Proteomics 5:835–844

De Jong-Brin M (1995) How schistosomes profit from the stress responses they elicit in their hosts. Adv Parasitol 35:177–256

Dillon GP, Feltwell T, Skelton J, Coulson PS, Wilson RA, Ivens AC (2008) Altered patterns of gene expression underlying the enhanced immunogenicity of radiation-attenuated schistosomes. PLoS Negl Trop Dis 2:e240

Eberl M, Langermans JA, Frost PA, Vervenne RA, van Dam GJ, Deelder AM, Thomas AW, Gorg A, Obermaier C, Boguth G, Harder A, Scheibe B, Wildgruber R, Weiss W (2000) The current state of two-dimensional electrophoresis with immobilized pH gradients. Electrophoresis 21:1037–1053

Görg A, Obermaier C, Boguth G, Harder A, Scheibe B, Wildgruber R, Weiss W (2000) The current state of two-dimensional electrophoresis with immobilized pH gradients. Electrophoresis 21:1037–1053

Guerra-Sa R, Castro-Borges W, Evangelista EA, Kettelhut IC, Rodrigues V (2005) Schistosoma mansoni: functional proteasomes are required for development in the vertebrate host. Exp Parasitol 109:228–236

Herbert B, Galvani M, Hamdan M, Olivieri E, MacCarthy J, Pedersen S, Righetti PG (2001) Reduction and alkylation of proteins in preparation of two-dimensional map analysis: why, when, and how? Electrophoresis 22:2046–2057

Hewitson JP, Hamblin PA, Mountford AP (2005) Immunity induced by the radiation-attenuated schistosome vaccine. Parasite Immunol 27:271–280

Hoffmann KF, Strand M (1996) Molecular identification of a Schistosoma mansoni tegumental protein with similarity to cytoplasmic dynein light chains. J Biol Chem 271:26117–26123

Hoffmann KF, Strand M (1997) Molecular characterization of a 20.8-kDa Schistosoma mansoni antigen. Sequence similarity to tegumental associated antigens and dynein light chains. J Biol Chem 272:14509–14515

Hu W, Yan Q, Shen DK, Liu F, Zhu ZD, Song HD, Xu XR, Wang ZJ, Rong YP, Zeng LC, Wu J, Zhang X, Wang JJ, Xu XN, Wang SY, Fu G, Zhang XL, Wang ZQ, Brindley PJ, McManus DP, Xue CL, Feng Z, Chen Z, Han ZG (2003) Evolutionary and biomedical implications of a Schistosoma japonicum complementary DNA resource. Nat Genet 35:139–147

Khalife J, Liu JL, Pierce R, Porchet E, Godin C, Capron A (1994) Characterization and localization of Schistosoma mansoni calreticulin Sm58. Parasitology 108(Pt 5):527–532

Knudsen GM, Medzihradszky KF, Lim KC, Hansell E, McKerrow JH (2005) Proteomic analysis of Schistosoma mansoni cercarial secretions. Mol Cell Proteomics 4:1862–1875

Kusel JR, Wales A, Vieira L, Wu KY (1989) Effects of irradiation and tunicamycin on the surface glycoproteins of Schistosoma-mansoni. Mem Inst Oswaldo Cruz 84:199–205

Liu F, Lu J, Hu W, Wang SY, Cui SJ, Chi M, Yan Q, Wang XR, Song HD, Xu XN, Wang JJ, Zhang XL, Zhang X, Wang ZQ, Xue CL, Brindley PJ, McManus DP, Yang PY, Feng Z, Chen Z, Han ZG (2006) New perspectives on host–parasite interplay by comparative transcriptomic and proteomic analyses of Schistosoma japonicum. PLoS Pathog 2:e29

Livak KJ, Schmittgen TD (2001) Analysis of relative gene expression data using real-time quantitative PCR and the 2(-Delta Delta C (T)) method. Methods 25:402–408

Loeffler IK, Bennett JL (1996) A rab-related GTP-binding protein in Schistosoma mansoni. Mol Biochem Parasitol 77:31–40

Mair GR, Maule AG, Fried B, Day TA, Halton DW (2003) Organization of the musculature of schistosome cercariae. J Parasitol 89:623–625

Maresca B, Carratu L (1992) The biology of the heat shock response in parasites. Parasitol Today 8:260–266

Mortz E, Krogh TN, Vorum H, Gorg A (2001) Improved silver staining protocols for high sensitivity protein identification using matrix-assisted laser desorption/ionization-time of flight analysis. Proteomics 1:1359–1363

Mountford AP, Harrop R (1998) Vaccination against schistosomiasis: the case for lung-stage antigens. Parasitol Today 14:109–114

Neumann S, Ziv E, Lantner F, Schechter I (1993) Regulation of HSP70 gene expression during the life cycle of the parasitic helminth Schistosoma mansoni. Eur J Biochem 212:589–596

Orlowski M, Wilk S (2003) Ubiquitin-independent proteolytic functions of the proteasome. Arch Biochem Biophys 415:1–5

Riengrojpitak S, Anderson S, Wilson RA (1998) Induction of immunity to Schistosoma mansoni: interaction of schistosomula with accessory leucocytes in murine skin and draining lymph nodes. Parasitology 117(Pt 4):301–309

Ruppel A, Shi YE, Moloney NA (1990) Schistosoma mansoni and S. japonicum: comparison of levels of ultraviolet irradiation for vaccination of mice with cercariae. Parasitology 101:23–26

Schmittgen TD, Zakrajsek BA (2000) Effect of experimental treatment on housekeeping gene expression: validation by real-time, quantitative RT-PCR. J Biochem Biophys Methods 46:69–81

Shi YE, Jiang CF, Han JJ, Li YL, Ruppel A (1990) Schistosoma japonicum: an ultraviolet-attenuated cercarial vaccine applicable in the field for water buffaloes. Exp Parasitol 71:100–106

Shi YE, Jiang CF, Han JJ, Li YL, Ruppel A (1993) Immunization of pigs against infection with Schistosoma japonicum using ultraviolet-attenuated cercariae. Parasitology 106(Pt 5):459–462

Srivastava P (2002) Roles of heat-shock proteins in innate and adaptive immunity. Nat Rev Immunol 2(3):185–194

Szumlewicz AP, Olivier LJ (1963) Schistosoma mansoni: development of challenge infections in mice exposed to irradiated cercariae. Science 140:411–412

Todryk SM, Melcher AA, Dalgleish AG, Vile RG (2000) Heat shock proteins refine the danger theory. Immunology 99(3):334–337

Torben W, Hailu A (2007) Serum cytokines of the 20 Krad-irradiated S. mansoni cercariae vaccinated, primary and superinfected Cercopethicus aethiops aethiops. Exp Parasitol 115:121–126

Villella JB, Gomberg HJ, Gould SE (1961) Immunization to Schistosoma mansoni in mice inoculated with radiated cercariae. Science 134:1073–1075

Wales A, Kusel JR (1992) Biochemistry of irradiated parasite vaccines—suggested models for their mode of action. Parasitol Today 8:358–363

Wales A, Kusel JR, Jones JT (1992) Inhibition of protein-synthesis in irradiated larvae of Schistosoma-mansoni. Parasite Immunol 14:513–530

Wiest PM, Burnham DC, Olds GR, Bowen WD (1992) Developmental expression of protein kinase C activity in Schistosoma mansoni. Am J Trop Med Hyg 46:358–365

Zugel U, Kaufmann SH (1999) Immune response against heat shock proteins in infectious diseases. Immunobiology 201(1):22–35